RSC Advances

ROYAL SOCIETY OF CHEMISTRY

PAPER

View Article Online
View Journal | View Issue

Check for updates

Cite this: *RSC Adv.*, 2025, **15**, 23097

1,2-Diaminocyclohexane-derived chiral tetradentate ligands for Mn(I)-catalyzed asymmetric hydrogenation of ketones†

Yi Su,‡[ab] Dongzhi Zhu,‡*[ac] Zhifeng Ma,‡*[cd] Yizhou Wang,[c] Zechen Wang,[b] Zheng Wang,*[bc] Yanping Ma[c] and Wen-Hua Sun*[c]

Received 1st May 2025
Accepted 20th June 2025

DOI: 10.1039/d5ra03062e

rsc.li/rsc-advances

A series of (*R*,*R*)-1,2-diaminocyclohexane-based chiral PNNP and SNNS tetradentate ligands were successfully employed as chiral chelating ligands for the asymmetric hydrogenation (AH) of substituted acetophenones (13 examples) with good activity and good enantioselectivity (up to 85% ee). In particular, two types of manganese(I) complexes (**Mn1** and **Mn2**) with a "C=N" or "NH" group were isolated, and their comparative performance as catalysts revealed **Mn1** as more effective in AH of ketones with a maximum enantiomeric excess (ee) value of 85%. DFT calculations revealed that the formation of the major S-type 1-phenylethanol by **Mn1** was significantly influenced by steric repulsion between the substrate and ligand.

Introduction

Catalytic asymmetric reduction of ketones to chiral alcohols with H_2 is of high academic and industrial interests owing to its widespread applications in many fields, such as in the production of drugs, pesticides, fragrances and other bioactive molecules.[1] Notably, most of the currently available successful catalysts are based on noble metals such as Ru,[2] Rh,[3] and Ir[4].[1a,5] However, the earth-abundance of the above metals is limited, and their use causes environmental pollution and safety concerns, promoting the search for alternative catalysts based on earth-abundant, base metals (Scheme 1a).[6] Consequently, AH catalysts based on manganese became particularly prominent owing to their high biocompatibility and earth-abundance.[7] Furthermore, with the continuous advancements in chiral ligand design methodologies, the application of manganese(I)-based chiral organometallic complexes in AH catalysis has been greatly promoted,[5a,b] and it has been receiving sustained attention from academic and industrial circles.[7] However, the activity and robustness of Mn-based catalytic systems generally fall short of those of noble metal-based catalytic systems.[7a,8]

In particular, Mn-based hydrogenation catalysis has become a subject of hot topic since 2016 when Beller's group first demonstrated its transformative potential in ketone

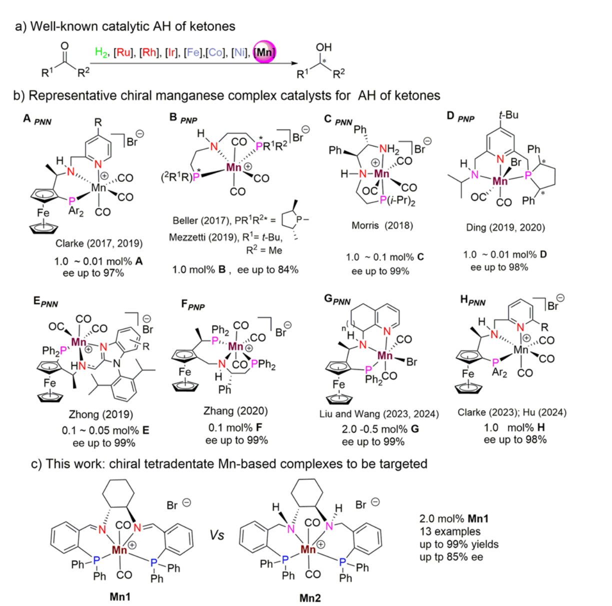

Scheme 1 (a) Various metal catalysts previously employed in the AH of ketones. (b) Selected tridentate-Mn(I) chiral catalysts for the AH of ketones; (c) Mn-based complexes studied in this work.

[a]Guangxi Key Laboratory of Advanced Structural Materials and Carbon Neutralization, School of Materials and Environment, Guangxi Minzu University, Nanning, 530105, China. E-mail: 20230021@gxmzu.edu.cn

[b]College of Science, Hebei Agricultural University, Baoding, 071001, China

[c]Key Laboratory of Engineering Plastics and Beijing National Laboratory for Molecular Science, Institute of Chemistry, Chinese Academy of Sciences, Beijing, 100190, China. E-mail: whsun@iccas.ac.cn; wangzheng@iccas.ac.cn

[d]School of Chemistry & Environment, Yunnan Key Laboratory of Chiral Functional Substance Research and Application, Yunnan Minzu University, Kunming, Yunnan, 650504, China. E-mail: mazhifeng@ymu.edu.cn

† Electronic supplementary information (ESI) available: Detailed experimental procedures, spectra (NMR, FT-IR), Fig. S1–S27, Chart S1, Tables S1–S8 and X-ray crystallographic data in CIF for CCDC 2408177 (**Mn1**). For ESI and crystallographic data in CIF or other electronic format see DOI: https://doi.org/10.1039/d5ra03062e

‡ These authors contributed equally.

hydrogenation.[9] Since then, the groups of Clarke,[10] Beller,[11] Ding,[12] Mezzetti,[13] Zhong,[14] Zhang,[15] Morris,[16] and Liu[17] *et al.*[18] have independently developed a series of Mn(I) complex catalysts (**A–H**, Scheme 1b), incorporating the chiral tridentate PNN or PNP ligands and successfully applying them in AH of ketones. Notably, the chiral 1,2-substituted ferrocene backbone was of particular interest. For example, Clarke *et al.* primarily described **A** bearing a ferrocene-incorporated chiral pincer ligand that could realize excellent turnover numbers (TONs up to 10 000) and offered chiral alcohols (ee up to 97%).[10a,b] Clarke's group further modified **A** to **H** for attaining compatibility with cyclic ketones, offering the corresponding chiral cyclic alcohols with ee up to 98%.[10c] More recently, Hu *et al.* reported **H** for the Mn-catalyzed AH of heterobiaryl ketone N-oxides with an enantiomeric excess of up to 99%.[18] Meanwhile, Zhong and co-workers developed a new chiral PNN catalyst (**E**) containing the "C=N" or "NH" group for AH of simple ketones and unsymmetrical benzophenones, offering an outstanding activity (up to 13 000 TON) and excellent enantioselectivities (>99% ee).[14] Zhang *et al.* demonstrated that **F** catalyzed the hydrogenation of ketones with excellent enantioselectivities (up to 99% ee) and high activity (up to 2000 TON).[15] We recently disclosed that strengthening the rigidity of the framework by adding the controllable "aliphatic cyclic" chiral amine motifs to a ferrocene moiety (**G**, Scheme 1b) can achieve the desired enantioinduction (up to 99% ee).[17] Despite these great advances, several limitations, such as poor availability of the starting materials for catalysts and limited types of catalysts, pose great challenges in the field of the manganese-catalyzed asymmetric reduction of ketones. Furthermore, the current Mn-based catalytic systems are mostly based on chiral pincer ligands. In contrast, tetradentate manganese(I) complexes were rarely reported.[19]

Typically, ruthenium-,[20] iron-,[6b,21] nickel-[22] and cobalt-[6f,23] based tetradentate complex catalysts exhibit excellent performance in the AH and asymmetric transfer hydrogenation (ATH) of ketones into chiral alcohols. Compared with bidentate and tridentate ligands, tetradentate ligands exhibit versatile features and effectively regulate the electronic and steric properties, bond angles, and catalytic performance of the formed catalysts.[24] In addition, tetradentate complex catalysts provide higher stability and unique chiral pocket towards carbonylation. Based on our long-term research interest in Mn-catalyzed (de)hydrogenation reactions,[25] herein, we report a series of (*R*,*R*)-1,2-diaminocyclohexane-based chiral tetradentate ligands (**L1–L4**) and two types of PNNP manganese(I) complexes with a "C=N" (**Mn1**) or "NH" (**Mn2**) group. Their comparative study on catalyst performance proved **Mn1** to be more effective in AH of ketones. Moreover, DFT calculations were used to understand the influence of C–N types (C=N (**Mn1**) *vs.* C–NH (**Mn2**)) and alkali-metal cations on the transition-state geometry of the hydrogen-transfer reaction. The distinct steric profiles of the C=N (planar) and C–NH (tetrahedral) configurations were found to critically influence the chiral pocket geometry, explaining the observed enantioselectivity trends and guiding our ligand optimization strategy.

Results and discussion

Based on the available literature,[20,26,27] 1,2-diaminocyclohexane-based chiral tetradentate ligands (**L1–L4**) were readily prepared *via* the condensation reaction between (*R*,*R*)-1,2-diaminocyclohexane and commercially available aldehydes or carboxylic acids, respectively (see ESI†). Subsequently, the four tetradentate ligands (**L1–L4**, see ESI†) containing chiral 1,2-diaminocyclohexane motif were explored for the Mn-catalyzed asymmetric hydrogenation of acetophenone (**a1**) in ethanol solution (Scheme 2). The catalyst was prepared by treating $Mn(CO)_5Br$ with 1.1 molar equivalents of the respective ligand in dry EtOH under reflux (80 °C, 4 h). The substrate and K_2CO_3 (as base) were dissolved in ethanol, followed by the addition of the EtOH solution to the *in situ* formed complex. In these AH tests, 2 mol% [**Mn**] with respect to acetophenone (**a1**) was employed, while 20 mol% K_2CO_3 was used as the base (Tables S1–S3, see ESI†). Notably, among these four *in situ* generated complexes, only the combination of $MnBr(CO)_5$/**L1** displayed higher activity (86% yield) for AH of **a1**, and the enantiomeric excess (ee) of **b1** regarding the chiral ligand (Scheme 2) dropped in the order of **L2** (70%) > **L1** (65%) > **L3** (45%) > **L4** (17%); this result aligned well with the previous finding reported by the groups of Gao and Li.[19a]

After identifying **L1** as the best ligand in the above tests, we proceeded to check the veracity of the complex structure and the catalytic process. Initial efforts focused on isolating the complex generated from the coordination reaction of $Mn(CO)_5Br$ with **L1** or **L2**. The P_2N_2-**Mn1** complex was efficiently prepared (84% yield) in toluene at 90 °C for 10 h, whereas P_2N_2-**Mn2** required reaction with dry toluene, refluxing for 12 h (Scheme 3a and see ESI†). Both P_2N_2-**Mn1** and P_2N_2-**Mn2** were characterized using $^1H/^{13}C/^{31}P$ NMR, elemental analysis, IR spectroscopy and crystal X-ray analysis. Notably, two strong peaks were displayed in the IR spectra at 1852 and 1950 cm^{-1}, which were characteristic of

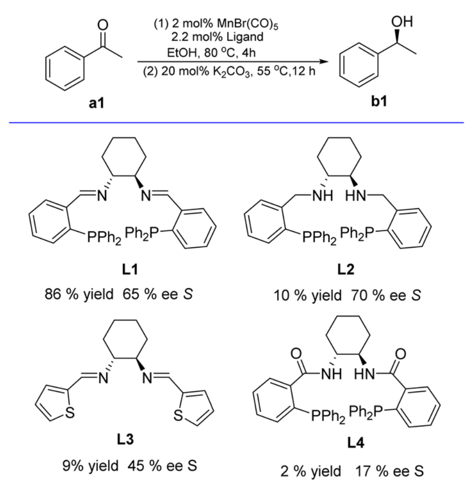

Scheme 2 Ligand screening. Conditions: (1) $Mn(CO)_5Br$ (2.0 mol%), **L1–L4** (2.2 mol%), 5 mL EtOH, 80 °C, 4 h; (2) **a1** (0.25 mmol), K_2CO_3 (20 mol%), 50 bar H_2, 55 °C, 12 h. Yields (%) and enantioselectivities (% ee) were determined using GC and chiral-phase GC, respectively, using a CP-Chirasil-Dex CB column.

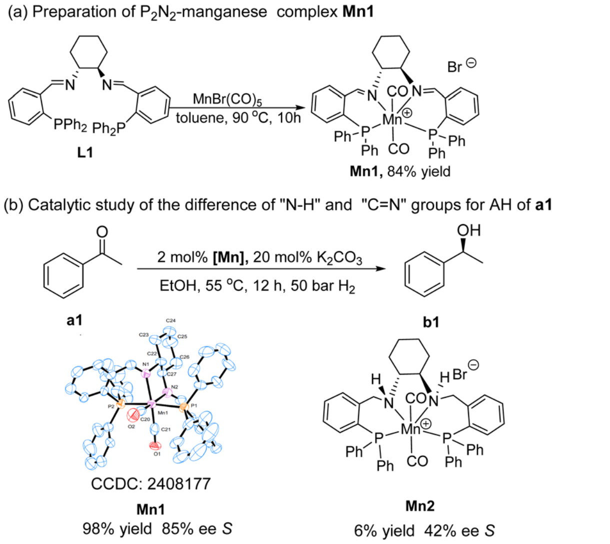

Scheme 3 Synthesis and reactivity of Mn(I) complexes Mn1 and Mn2.

CO ligands coordinated to manganese in each complex. Additionally, **Mn1** exhibited a prominent peak at 1612 cm^{-1}, matching the expected C═N stretching frequency. In contrast, **Mn2**'s IR spectrum displayed strong absorption bands around 1622 cm^{-1} and 3233 cm^{-1}, which corresponded to the NH group.

Meanwhile, their ^{31}P NMR spectra (recorded in DMSO-d_6) offered key structural insights, with the phosphine signal for **Mn1** appearing at 63.45 ppm and at 61.93 ppm for **Mn2** (*cf.* δ −13.68 ppm for **L1** and δ −15.92 ppm for **L2**). Furthermore, single crystals of **Mn1** were successfully obtained for X-ray diffraction analysis, confirming its molecular structure. Crystallographic data revealed that the cationic unit of **Mn1** (Scheme 3b and Table S4,† CCDC: 2408177) adopted a distorted octahedral geometry in the *P*3121 space group, in which the two imine moieties and carbonyl groups were coordinated in a *cis*-fashion, while the two phosphine groups were bound in a *trans*-fashion to each other. Structural parameters, including bond lengths and angles for **Mn1**, are summarized in Table S5 (see ESI†).

Structural comparison between **Mn1** and a reported achiral cyclic manganese(I) complex **Mn3**,[19b] exhibited difference in their structures with respect to bond distances (Table 1). **Mn1** contained two unsaturated C═N bonds. The N1–C19 and N2–C28 bond distances of 1.238(9) Å and 1.242(9) Å, respectively, were typical of C═N distances. As for the case of the complex **Mn3** reported by Fang *et al.*,[19b] both C–N bonds demonstrated lengths of typical saturated covalent connections. **Mn1** has Mn–N bonds of 2.081(6) Å and 2.078(6) Å, while the reported complex **Mn3** exhibited longer Mn–N bonds of 2.161(7) Å and 2.143(6) Å. **Mn1** also exhibited shorter Mn–P bonds than **Mn3** [2.308(2) Å and 2.322(2) Å *vs.* 2.293(2) Å and 2.269(2) Å]. **Mn1** displayed greater steric encumbrance in its cyclic arrangement than **Mn3** owing to its rigid C═N connectivity. Accordingly, **Mn3** displayed higher activity for the hydrogenation of ketones.[19b] Currently, few examples exist for these carefully constructed chiral manganese(I) cyclic complexes with P_2N_2 donor sets. When applied to acetophenone (**a1**) hydrogenation (Scheme 3b), **Mn1** showed remarkable catalytic activity (98% conversion) and stereoselectivity (85% ee), significantly outperforming **Mn2** (6% yield, 42% ee). This difference underscores the critical role of imine functionality in the cyclohexanediamine-derived ligand framework for effective metal–ligand cooperative catalysis.[14a]

Table 1 Selected experimental bond distances (Å) for Mn1 and the reported achiral cyclic manganese(I) complex Mn3

Complex	N–C (Å)	Mn–N (Å)	Mn–P (Å)
Mn1	N1–C19 1.238(9)	**Mn1**–N1 2.081(6)	**Mn1**–P1 2.293(2)
	N2–C28 1.242(9)	**Mn1**–N2 2.078(6)	**Mn1**–P2 2.269(2)
Mn3,[19b]	N1–C01V 1.50(1)	**Mn1**–N1 2.161(7)	**Mn1**–P1 2.308(2)
	N2–C016 1.483(9)	**Mn1**–N2 2.143(6)	**Mn1**–P2 2.322(2)

With the best manganese complex catalyst in hand, we decided to explore **Mn1** as a catalyst for the benchmark AH transformation of acetophenone (**a1**) to *S*-1-phenylethanol (**b1**). Initial optimization attempts revealed that **Mn1** (2 mol%, S/C = 50) combined with *t*-BuOK (20 mol%) at 55 °C produced **b1** in near-quantitative yield (99%), with 65% ee (entry 1, Table S1, see ESI†). With the aim to establish the most compatible base, the AH of **a1** was then screened for various bases, including *t*-BuOK, *t*-BuONa, *t*-BuOLi, CH_3ONa, K_3PO_4, KOH, NaOH, $LiOH\cdot H_2O$, K_2CO_3, and Cs_2CO_3 in EtOH at 55 °C (Table S1, see ESI†). As shown in Fig. 1, both the yields and enantioselectivity were strongly dependent on the selected alkali metal cation. Among them, K^+ offered the greatest promoting effect, *viz.*, K_2CO_3 proved as a standout example (ee ≥ 85%) owing to its moderate alkalinity and better compatibility between the size of the potassium ion and ligand's cavity.

Considering the importance of temperature on catalytic activity and enantioselectivity, the AH of **a1** was systematically investigated at temperatures ranging from 35 °C to 85 °C, with K_2CO_3 employed consistently as the base (Table S3, see ESI†).

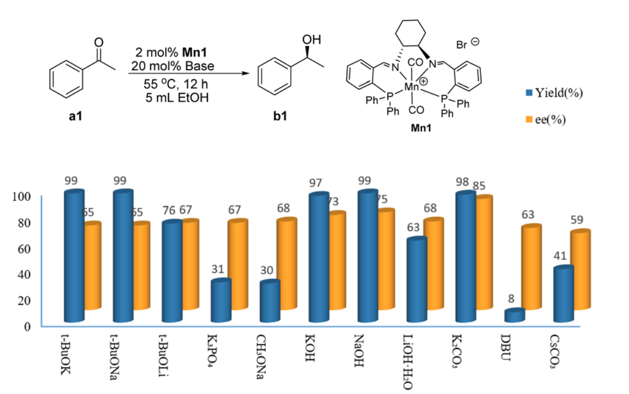

Fig. 1 Screening of bases. Conditions: 0.25 mmol **a1**, 0.05 mmol base (20 mol%), 5 μmol **Mn1** (2 mol%), 50 bar H_2, 5 mL EtOH, 55 °C, 12 h; yields (%) and enantioselectivities (% ee) were determined using GC and chiral-phase GC, respectively, using a CP-Chirasil-Dex CB column.

Notably, excellent conversions to **b1** in the range of 97% to 99% were observed across the temperature range from 55 °C to 85 °C. However, a lower temperature (45 °C) was found to be unfavorable for the transformations, with a distinct loss in conversion observed at 45 °C, which can attributed to the fact that low temperature could not overcome the energy barrier. Furthermore, enantioselectivity with a distinct loss in selectivity was observed at 75 °C.

With the standard reaction conditions (2 mol% **Mn1**, 20 mol% K_2CO_3, 55 °C, EtOH) in hand, we further explored the capacity of this Mn-based catalytic system for the AH of ketones (Table 2). Various acetophenones and their derivatives (**a2–a15**) were explored for the AH of ketones. In general, substituted acetophenones containing electron-withdrawing substituents (Cl and Br: **a3–a4**, **a7–a8** and **a11–a12**) displayed higher activities and diminished optical purities than their analogues containing electron-donating methyl groups (Me: **a5**, **a9** and **a13**). Notably, the pattern of substituents on the phenyl ring exhibited a significant influence on the conversion of the product, and steric hindrance on the ortho-position (**b2–b5**) led to a decrease in the yield. In terms of steric effects, enhanced steric hindrance on the aromatic ring (*e.g.* 2,6-disubstituted **b14** and **b15**) led to trace product conversions. Furthermore, the results showed that enantio-selectivities decreased in the sequence of *meta* (58–79% ee) > *para* (65–72% ee) > *ortho* (27–68% ee). Compared with the reported manganese complex catalysts (**A**, **C**, **D**, **E**, **F** and **H**), the current system based on **Mn1** displayed lower activities and lower enantioselectivities for the substituted acetophenones.

Based on the bifunctional concept,[6f,7b,22c] and our early mechanistic studies,[17] DFT calculations using the PCM B3LYP-D3//B3LYP-D3 method were performed to investigate the influence of the types of C–N bonds (imine C=N in **Mn1** *vs.* amine C–NH in **Mn2**) and potassium cations on the transition-state geometry during hydrogen transfer (see Tables S6–S8†). Results revealed that the free energy barriers for hydrogen atom transfer (HAT) in the generation of (S)-type chiral product with **Mn1** and **Mn2** catalyst were lower than those for (R)-type chiral product, with a $\Delta\Delta G$ of 1.4 and 0.7 kcal mol^{-1}, respectively (Fig. 2a and b). The distortion energy ($\Delta\Delta\ E_{dist}$ ~4.5 kcal mol; Fig. 2c) played a key role in controlling the enantioselectivity (% V_Burs = 76.7 and 75.3 for **TSR$_{Mn1}$** and **TSS$_{Mn1}$**, respectively). In contrast, the noncovalent interaction (π–π stacking) played a key role in controlling the enantioselectivity of **TSR$_{Mn2}$** and **TSS$_{Mn2}$** ($\Delta\Delta\ E_{int}$ = ~6.0 kcal mol; Fig. 2d). In comparison to the (S)-type chiral product generated with the **Mn2** catalyst, the formation of the (S)-product catalyzed by **Mn1** was favored through the transition state **TSS$_{Mn1}$**. The observed free-energy difference ($\Delta\Delta G$ = ~3.4 kcal mol^{-1}) primarily stemmed from

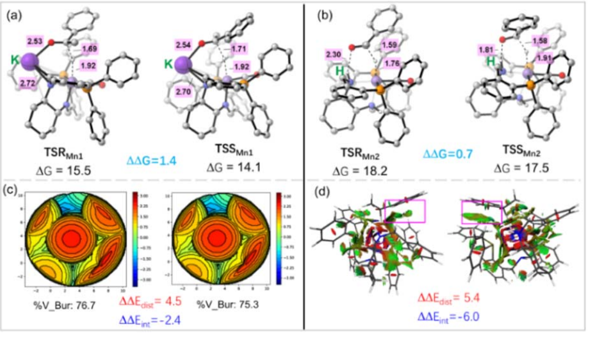

Fig. 2 Bond distances (in Å) and corrected Gibbs free energies (in kcal mol^{-1}) of transition states (**TSs**) calculated using the PCM B3LYP-D3/SDD+6-311+G**//B3LYP-D3/SDD+6-31G* method in an ethanol solution: (a) **TS** involving K^+ ion derived from **Mn1**; (b) **TS** derived from **Mn2**; (c) distortion–interaction energy analysis of the transition states, showing the distortion energy ($\Delta\Delta E_{dist}$) and interaction energy ($\Delta\Delta E_{int}$) between acetone and the remaining Mn-**L1** parts, the steric map with the computed buried volumes (in %); and (d) noncovalent interaction (NCI) plots (red: strong repulsion; green: weak attraction; blue: strong attraction).

Table 2 Scope of the AH of substituted acetophenones[a]

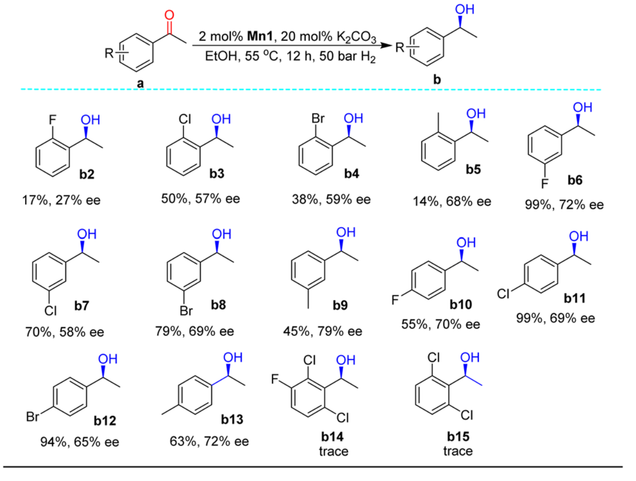

[a] Conditions: 0.25 mmol ketone (**a1–a15**), 0.05 mmol K_2CO_3 (20 mol%), 5 μmol **Mn1** (2 mol%), 50 bar H_2, 5 mL EtOH, 55 °C, 12 h. Yields (%) and enantioselectivities (% ee) were determined using GC and chiral-phase GC, respectively.

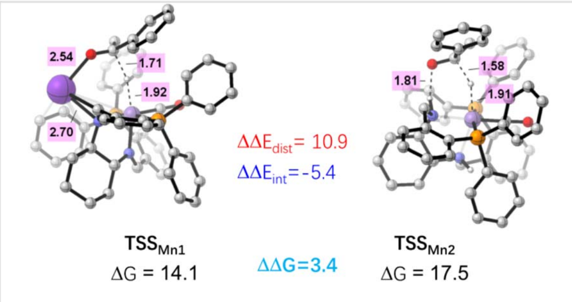

Fig. 3 Relative corrected free energies (in kcal mol^{-1}) for $\mathbf{TSS_{Mn1}}$ and $\mathbf{TSS_{Mn2}}$ calculated using the PCM B3LYP-D3/BS2//B3LYP-D3/BS1 method in an ethanol solution.

the steric interactions between the ketone substrate (**a1**) and catalyst ($\Delta\Delta E_{\rm dist}$ ~10.9 kcal mol; Fig. 3). In general, the DFT results indicated that the generation of the major S-type product by **Mn1** with good ee values was mainly influenced by the steric repulsion between the substrate and ligand. Our DFT results were consistent with the experimental observations.

Conclusions

In conclusion, we have successfully synthesized a series of chiral tetradentate ligands and two new coordination P_2N_2 manganese(I) complexes with "C═N" (**Mn1**) or "NH" (**Mn2**) groups and demonstrated their successful applications in the AH of aryl and alkyl ketones. Applying **Mn1**, featuring a (*R*,*R*)-1,2-diaminocyclohexane scaffold, high activity and good stereocontrol (up to 85% ee) were achieved across diverse acetophenone derivatives to produce enantio-enriched 1-phenylethanols. DFT calculations revealed that the origin of the distinctive anti stereoselectivity in the catalysis was mainly owing to the steric repulsion between the substrate and ligand in the favored transition state. Further investigations on the reaction mechanism are currently ongoing in our laboratory.

Data availability

The data that support the findings of this study are available in the ESI† of this article.

Conflicts of interest

There are no conflicts to declare.

Acknowledgements

D. Z. would like to acknowledge the financial support from the Nature Science Foundation of Guangxi Province (2024JJB120135). Z. W. acknowledge the support from the Hebei provincial central guiding local science and Technology Development Fund project (236Z1402G). Z. W. would like to acknowledge the financial support from the Hebei Graduate Innovation Funding Project (CXZZSS20250041). Z. M and Z. W. would like to acknowledge the financial support from the Yunnan Key Laboratory of Chiral Functional Substance Research and Application (202402AN360010; 2024SXFKO5).

References

1 (*a*) V. Ratovelomanana-Vidal and P. Phansavath, *Asymmetric hydrogenation and transfer hydrogenation*, Wiley-VCH, 2021; (*b*) P.-C. Yan, G.-L. Zhu, J.-H. Xie, X.-D. Zhang, Q.-L. Zhou, Y.-Q. Li, W.-H. Shen and D.-Q. Che, *Org. Process Res. Dev.*, 2013, **17**, 307–312; (*c*) G.-L. Zhu, X.-D. Zhang, L.-J. Yang, J.-H. Xie, D.-Q. Che, Q.-L. Zhou, P.-C. Yan and Y.-Q. Li, *Org. Process Res. Dev.*, 2015, **20**, 81–85; (*d*) S. Duan, B. Li, R. W. Dugger, B. Conway, R. Kumar, C. Martinez, T. Makowski, R. Pearson, M. Olivier and R. Colon-Cruz, *Org. Process Res. Dev.*, 2017, **21**, 1340–1348.

2 (*a*) M. Kitamura, T. Ohkuma, S. Inoue, N. Sayo, H. Kumobayashi, S. Akutagawa, T. Ohta, H. Takaya and R. Noyori, *J. Am. Chem. Soc.*, 2002, **110**, 629–631; (*b*) R. N. A. T. Ohkuma, *Angew. Chem., Int. Ed.*, 2001, **40**, 40–73; (*c*) K. Matsumura, N. Arai, K. Hori, T. Saito, N. Sayo and T. Ohkuma, *J. Am. Chem. Soc.*, 2011, **133**, 10696–10699; (*d*) F. Naud, F. Spindler, C. J. Rueggeberg, A. T. Schmidt and H. U. Blaser, *Org. Process Res. Dev.*, 2007, **11**, 519–523; (*e*) Y. Li, K. Ding and C. A. Sandoval, *Org. Lett.*, 2009, **11**, 907–910; (*f*) T. Ohkuma and N. Arai, *Chem. Rec.*, 2016, **16**, 2797–2815.

3 (*a*) H. Nie, G. Zhou, Q. Wang, W. Chen and S. Zhang, *Tetrahedron: Asymmetry*, 2013, **24**, 1567–1571; (*b*) D.-H. Bao, H.-L. Wu, C.-L. Liu, J.-H. Xie and Q.-L. Zhou, *Angew. Chem., Int. Ed.*, 2015, **54**, 8791–8794; (*c*) F.-H. Zhang, F.-J. Zhang, M.-L. Li, J.-H. Xie and Q.-L. Zhou, *Nat. Catal.*, 2020, **3**, 621–627; (*d*) S. F. Zhu and Q. L. Zhou, *Acc. Chem. Res.*, 2017, **50**, 988–1001; (*e*) F. Yang, J. H. Xie and Q. L. Zhou, *Acc. Chem. Res.*, 2023, **56**, 332–349; (*f*) K. Chang, L. Yang, Y. Liu, J. Cao, L. Zuo, Q. Liu, X. Zhang, C. Yin and H. Zhou, *Org. Lett.*, 2024, **26**, 9841–9846.

4 (*a*) H. Yang, N. Huo, P. Yang, H. Pei, H. Lv and X. Zhang, *Org. Lett.*, 2015, **17**, 4144–4147; (*b*) F. Bruning, H. Nagae, D. Kach, K. Mashima and A. Togni, *Chem.–Eur. J.*, 2019, **25**, 10818–10822; (*c*) H. Sun, L. Xu, S. Ruan, V. Ratovelomanana-Vidal, G. Q. Chen and X. Zhang, *Org. Lett.*, 2024, **26**, 10008–10012.

5 (*a*) H. Wang, J. Wen and X. Zhang, *Chem. Rev.*, 2021, **121**, 7530–7567; (*b*) D. H. Liang, C. J. Hou, Q. Li, H. Qin, L. Li and X. P. Hu, *Adv. Synth. Catal.*, 2024, **366**, 2165–2185.

6 (*a*) T. Zell and R. Langer, *ChemCatChem*, 2018, **10**, 1930–1940; (*b*) Y.-Y. Li, S.-L. Yu, W.-Y. Shen and J.-X. Gao, *Acc. Chem. Res.*, 2015, **48**, 2587–2598; (*c*) G. A. Filonenko, R. van Putten, E. J. M. Hensen and E. A. Pidko, *Chem. Soc. Rev.*, 2018, **47**, 1459–1483; (*d*) F. Kallmeier and R. Kempe, *Angew. Chem., Int. Ed.*, 2018, **57**, 46–60; (*e*) P. Wang, Z. L. He, Z. F. Xia, J. Wei and X. Q. Dong, *Chin. J. Chem.*, 2024, **42**, 3135–3156; (*f*) Z. Wang, M. Li and W. Zuo, *J. Am. Chem. Soc.*, 2024, **146**, 26416–26426.

7 (*a*) D. Fu, Z. Wang, Q. Liu, S. Prettyman, G. A. Solan and W.-H. Sun, *ChemCatChem*, 2024, e202301567; (*b*) K. Das, S. Waiba, A. Jana and B. Maji, *Chem. Soc. Rev.*, 2022, **51**, 4386–4464.

8 (*a*) C. Liu, R. van Putten, P. O. Kulyaev, G. A. Filonenko and E. A. Pidko, *J. Catal.*, 2018, **363**, 136–143; (*b*) W. Yang, T. Y. Kalavalapalli, A. M. Krieger, T. A. Khvorost, I. Y. Chernyshov, M. Weber, E. A. Uslamin, E. A. Pidko and G. A. Filonenko, *J. Am. Chem. Soc.*, 2022, **144**, 8129–8137; (*c*) W. Yang, E. Nieuwlands, I. Y. Chernyshov, G. A. Filonenko and E. A. Pidko, *ChemCatChem*, 2025, **17**, e202401237.

9 S. Elangovan, C. Topf, S. Fischer, H. Jiao, A. Spannenberg, W. Baumann, R. Ludwig, K. Junge and M. Beller, *J. Am. Chem. Soc.*, 2016, **138**, 8809–8814.

10 (*a*) M. B. Widegren, G. J. Harkness, A. M. Z. Slawin, D. B. Cordes and M. L. Clarke, *Angew. Chem., Int. Ed.*, 2017, **56**, 5825–5828; (*b*) M. B. Widegren and M. L. Clarke, *Catal. Sci. Technol.*, 2019, **9**, 6047–6058; (*c*) C. L. Oates, A. S. Goodfellow, M. Buhl and M. L. Clarke, *Angew. Chem., Int. Ed.*, 2023, **62**, e202212479.

11 M. Garbe, K. Junge, S. Walker, Z. Wei, H. Jiao, A. Spannenberg, S. Bachmann, M. Scalone and M. Beller, *Angew. Chem., Int. Ed.*, 2017, **56**, 11237–11241.

12 (*a*) L. Zhang, Y. Tang, Z. Han and K. Ding, *Angew. Chem., Int. Ed.*, 2019, **58**, 4973–4977; (*b*) L. Zhang, Z. Wang, Z. Han and K. Ding, *Angew. Chem., Int. Ed.*, 2020, **59**, 15565–15569.

13 A. Passera and A. Mezzetti, *Adv. Synth. Catal.*, 2019, **361**, 4691–4706.

14 (*a*) F. Ling, H. Hou, J. Chen, S. Nian, X. Yi, Z. Wang, D. Song and W. Zhong, *Org. Lett.*, 2019, **21**, 3937–3941; (*b*) F. Ling, J. Chen, S. Nian, H. Hou, X. Yi, F. Wu, M. Xu and W. Zhong, *Synlett*, 2020, **31**, 285–289; (*c*) Z. Wang, X. Zhao, A. Huang, Z. Yang, Y. Cheng, J. Chen, F. Ling and W. Zhong, *Tetrahedron Lett.*, 2021, **82**, 153389; (*d*) J. He, W. Mao, J. Lin, Y. Wu, L. Chen, P. Yang, D. Song, P. Zhu, W. Zhong and F. Ling, *Org. Chem. Front.*, 2023, **10**, 3321–3327.

15 L. Zeng, H. Yang, M. Zhao, J. Wen, J. H. R. Tucker and X. Zhang, *ACS Catal.*, 2020, **10**, 13794–13799.

16 C. S. G. Seo, B. T. H. Tsui, M. V. Gradiski, S. A. M. Smith and R. H. Morris, *Catal. Sci. Technol.*, 2021, **1**, 3153–3163.

17 (*a*) J. Yang, L. Yao, Z. Wang, Z. Zuo, S. Liu, P. Gao, M. Han, Q. Liu, G. A. Solan and W.-H. Sun, *J. Catal.*, 2023, **418**, 40–50; (*b*) Y. Su, Z. Ma, J. Wang, L. Li, X. Yan, N. Ma, Q. Liu, G. A. Solan and Z. Wang, *J. Org. Chem.*, 2024, **89**, 12318–12325; (*c*) Z. Wang, S. Zhang, Z. Ma, L. Li, X. Yan, Q. Cao, Y. Su, N. Ma and Z. Wang, *Mol. Catal.*, 2024, **564**, 114274; (*d*) S. Zhang, Z. Ma, Y. Li, Y. Su, N. Ma, X. Guo, L. Li, Q. Liu and Z. Wang, *J. Catal.*, 2024, **437**, 115682.

18 Y.-B. Wan and X.-P. Hu, *ACS Catal.*, 2024, **14**, 17633–17641.

19 (*a*) G.-Y. Zhang, S.-H. Ruan, Y.-Y. Li and J.-X. Gao, *Chin. Chem. Lett.*, 2021, **32**, 1415–1418; (*b*) Y. Zhang, B. Li, T. Wang, N. Duan, J. Zheng, H. Li, F. Zhang and X. Fang, *Dalton Trans.*, 2024, **53**, 16475–16479.

20 (*a*) J.-X. Gao, T. Ikariya and R. Noyori, *Organometallics*, 1996, **15**, 1087–1089; (*b*) H. Zhang, C. B. Yang, Y. Y. Li, Z. R. Donga, J. X. Gao, H. Nakamura, K. Murata and T. Ikariya, *Chem. Commun.*, 2003, **1**, 142–143.

21 (*a*) W. Zuo, A. J. Lough, Y. F. Li and R. H. Morris, *Science*, 2013, **342**, 1080–1083; (*b*) Y. Li, S. Yu, X. Wu, J. Xiao, W. Shen, Z. Dong and J. Gao, *J. Am. Chem. Soc.*, 2014, **136**, 4031–4039; (*c*) R. Bigler, R. Huber and A. Mezzetti, *Angew. Chem., Int. Ed.*, 2015, **54**, 5171–5174; (*d*) K. Z. Demmans, C. S. G. Seo, A. J. Lough and R. H. Morris, *Chem. Sci.*, 2017, **8**, 6531–6541; (*e*) Q. Xue, R. Wu, D. Wang, M. Zhu and W. Zuo, *Organometallics*, 2020, **40**, 134–147; (*f*) R. T. Endean, L. Rasu and S. H. Bergens, *ACS Catal.*, 2019, **9**, 6111–6117.

22 (*a*) Z. R. Dong, Y. Y. Li, S. L. Yu, G. S. Sun and J. X. Gao, *Chin. Chem. Lett.*, 2012, **23**, 533; (*b*) Z. Wang, S.-L. Yu, Z.-B. Wei, D.-L. An, Y.-Y. Li and J.-X. Gao, *J. Organomet. Chem.*, 2019, **898**, 120882; (*c*) H. Chen, Z. Wang, M. Li and W. Zuo, *ACS Catal.*, 2023, **13**, 4261.

23 (*a*) M. Li, Z. Wang, H. Chen, Q. Huang and W. Zuo, *Chem*, 2024, **10**, 250–264; (*b*) S.-H. Ruan, Z.-W. Fan, W.-J. Zhang, H. Xu, D.-L. An, Z.-B. Wei, R.-M. Yuan, J.-X. Gao and Y.-Y. Li, *J. Catal.*, 2023, **418**, 100–109.

24 (*a*) W. Li, J.-H. Xie, M.-L. Yuan and Q.-L. Zhou, *Green Chem.*, 2014, **16**, 4081–4085; (*b*) X. Tan, Y. Wang, Y. Liu, F. Wang, L. Shi, K. H. Lee, Z. Lin, H. Lv and X. Zhang, *Org. Lett.*, 2015, **17**, 454–457; (*c*) U. Sharma, N. Kumar, P. K. Verma, V. Kumar and B. Singh, *Green Chem.*, 2012, **14**, 2289–2293; (*d*) P. K. Verma, U. Sharma, N. Kumar, M. Bala, V. Kumar and B. Singh, *Catal. Lett.*, 2012, **142**, 907–913; (*e*) P. K. Verma and S. D. Sawant, *Coord. Chem. Rev.*, 2022, **450**, 214239.

25 (*a*) Z. Wang, Q. Lin, N. Ma, S. Liu, M. Han, X. Yan, Q. Liu, G. A. Solan and W.-H. Sun, *Catal. Sci. Technol.*, 2021, **11**, 8026–8036; (*b*) Z. Wang, N. Ma, X. Lu, M. Liu, T. Liu, Q. Liu, G. A. Solan and W.-H. Sun, *Dalton Trans.*, 2023, **52**, 10574–10583; (*c*) D. Fu, Z. Wang, M. Liu, S. Liu, Y. Wang, C. Wei, Y. Ma, Q. Liu, G. A. Solan and W.-H. Sun, *J. Catal.*, 2024, **436**, 115601; (*d*) Z. Wang, X. Lu, Z. Li, L. Li, Z. Ma, N. Ma, X. Yan, X. Liu, P. Han and Q. Liu, *J. Catal.*, 2024, **430**, 115337.

26 X.-Q. Zhang, Y.-Y. Li, Z.-R. Dong, W.-Y. Shen, Z.-B. Cheng and J.-X. Gao, *J. Mol. Catal. A:Chem.*, 2009, **307**, 149–153.

27 (*a*) M. Cettolin, P. Puylaert, L. Pignataro, S. Hinze, C. Gennari and J. G. de Vries, *ChemCatChem*, 2017, **9**, 3125–3130; (*b*) Y. Zhang, E. Chong, J. A. H. White, S. Radomkit, Y. Xu, S. C. Kosnik and J. C. Lorenz, *Synlett*, 2022, **33**, 1287–1289.